© IIJP 2026 | Volume 2, Issue 3, pp. 2005-2025 | ISSN: 2636-4484

EFFICACY OF SELECTED SEED EXTRACTS AND GREEN SYNTHESIZED MAGNESIUM OXIDE NANOPARTICLES IN THE REMEDIATION OF CONTAMINATED WATER

***Iornumbe Sandra Mnguhenen[1], Thomas Okoh[2], Olasan Olalekan Joseph[3], Aguoru, Celestine Uzoma[4], Tivkaa Terfa Joseph[5] & Ihekwoaba Chiamaka Chinomso[6]**

[1]*Department of Science Laboratory Technology, Benue State Polytechnic, Ugbokolo, Nigeria.*
[2,3,4]*Department of Plant Science and Biotechnology, Joseph Sarwuan Tarka University, Makurdi, Nigeria.*
[5]*Department of Science Laboratory Technology, Benue State Polytechnic, Ugbokolo, Nigeria.*
[6]*Department of General Studies, Federal Polytechnic, Ugep, Cross River State, Nigeria.*
***Corresponding author:** iornumbesandra2017@gmail.com

ARTICLE INFO
Article No.: 0566
Accepted Date: 17/08/2026
Published Date: 11/09/2026
Type: Research

ABSTRACT

Background: Heavy-metal contamination threatens water safety, while conventional treatment methods may be costly in resource-constrained settings. Plant seed powders and green-synthesized magnesium oxide nanoparticles (MgONPs) offer affordable remediation materials.

Gap: Evidence comparing moringa, pawpaw and orange seed powders with MgONPs, applied individually and in combinations and evaluated using metal-specific removal and the Heavy Metal Pollution Index (HPI), remains limited.

Aim: This study compared the remediation performance of seed powders and green-synthesized MgONPs in multi-metal-contaminated water.

Methods: MgONPs synthesized using *Jatropha tanjorensis* leaf extract were characterized by ultraviolet-visible spectroscopy, Fourier-transform infrared spectroscopy, scanning electron microscopy, energy-dispersive X-ray spectroscopy and X-ray diffraction. Fifteen individual and combined treatments and two controls were evaluated in triplicate for physicochemical properties, nutrients and Cd, Ni, Pb, Hg and Ag. Removal efficiencies and HPI were calculated, and treatment patterns were examined using hierarchical cluster analysis.

Results: Treatment effects varied significantly across physicochemical properties and metals. Pawpaw-orange achieved the strongest broad-spectrum remediation, removing 98.26% Cd, 100% Pb, 99.41% Hg and 100% Ag and recording the lowest HPI (0.211). Pawpaw-MgONPs produced the greatest Ni removal (98.34%). In contrast, MgONPs-orange had an HPI of 2.359 and was not classified as remediated. Several combinations, particularly the complete mixture, increased dissolved and suspended solids, electrical conductivity, hardness and biochemical oxygen demand, demonstrating that metal removal did not necessarily improve water quality.

Conclusion: Seed powders and MgONPs showed treatment-specific remediation potential. Pawpaw-orange was the most promising treatment, but dosage optimization, adsorbent recovery, post-treatment filtration and safety evaluation are required before practical drinking-water application.

Keywords: Heavy metals; water remediation; seed powders; magnesium oxide nanoparticles; green synthesis; Heavy Metal Pollution Index.

Introduction

Safe water is essential for human health, food production, sanitation and socioeconomic development (World Health Organization [WHO], 2022). However, freshwater resources are increasingly contaminated through mining, industrial effluents, sewage discharge, agricultural runoff, waste disposal and corrosion of metal-containing materials (Hasan et al., 2020). Heavy metals are particularly concerning because they are persistent, non-biodegradable and capable of accumulating in organisms and food chains (Sharma & Bhattacharya, 2017). Exposure to Cd, Ni, Pb, Hg and Ag has been associated with renal, neurological, cardiovascular, skeletal and other systemic effects, although their toxicity varies with concentration, chemical form and exposure duration (Jaishankar et al., 2014; Genchi et al., 2020).

Conventional heavy-metal removal methods include chemical precipitation, coagulation, ion exchange, membrane filtration, electrochemical treatment and adsorption (Qasem et al., 2021). Despite their effectiveness, some methods require expensive materials and substantial energy inputs, while others generate toxic sludge or experience membrane fouling, incomplete metal removal and difficulties treating mixtures of competing ions (Barakat, 2011). These limitations have increased interest in affordable and environmentally sustainable treatment materials, particularly for resource-constrained communities (Koul et al., 2022).

Plant-based coagulants and biosorbents contain proteins, polysaccharides and functional groups that support coagulation, floc formation and contaminant adsorption (Hegazy et al., 2021). *Moringa oleifera* seeds contain cationic proteins that neutralize negatively charged particles, while their amino, carboxyl and hydroxyl groups provide binding sites for dissolved metal ions (Camacho et al., 2017). Moringa seed biomass has demonstrated the removal of Pb, Ni and Cd, although its performance depends on pH, dosage and initial metal concentration (Aziz et al., 2016).

Carica papaya seeds possess proteins, charged surfaces and functional groups that promote particle destabilization, interparticle bridging and pollutant adsorption (Amran et al., 2021). Papaya seed treatment has produced reductions in turbidity, suspended contaminants, nitrate and indicator bacteria in polluted water (Adekitan et al., 2023). Orange (*Citrus sinensis*) seed powder contains protein and fibre-rich constituents that may provide functional sites for contaminant adsorption (Parobali et al., 2024). Orange seed powder has reduced turbidity, suspended solids and organic pollution in water and has demonstrated biosorption capacity in textile wastewater (Flores Alarcón et al., 2022). The availability, biodegradability and relatively low cost of these seeds support their application as locally sourced water-treatment materials (Unnisa & Bi, 2018).

Metal-oxide nanoparticles possess large reactive surfaces that facilitate adsorption, precipitation and catalytic degradation of water contaminants (Ghoniem et al., 2022). MgONPs can adsorb dissolved metals and inhibit bacteria through reactive oxygen species production, membrane disruption and direct nanoparticle–cell interaction (Cai et al., 2017; He et al., 2016). Green synthesis uses plant-derived compounds to facilitate nanoparticle formation and stabilization while reducing dependence on hazardous synthetic reagents (Rotti et al., 2023). Consequently, green-synthesized MgONPs may combine effective contaminant removal with a more environmentally compatible production process (Muhaymin *et al*., 2024).

Previous studies have largely investigated moringa, pawpaw, orange seeds and MgONPs separately and under different experimental conditions, thereby limiting direct comparison of their remediation efficiencies. Evidence on their combined application for removing multiple heavy metals remains limited, particularly when seed-seed and seed-nanoparticle treatments are compared within the same experiment. Few studies have also integrated physicochemical water

quality, individual removal of Cd, Ni, Pb, Hg and Ag, and the Heavy Metal Pollution Index in evaluating treatment performance.

Aim and Objectives of the Study

This study aimed to evaluate the effectiveness of selected seed powders and green-synthesized magnesium oxide nanoparticles (MgONPs), applied individually and in combination, for remediating heavy metal-contaminated water. The specific objectives were to:

1. 1. Synthesize and characterize MgONPs produced using *Jatropha tanjorensis* leaf extract;
2. 2. Compare the effects of individual and combined seed-powder and MgONP treatments on the physicochemical properties and concentrations of Cd, Ni, Pb, Hg and Ag in contaminated water; and
3. 3. Determine the heavy-metal removal efficiencies and Heavy Metal Pollution Index (HPI) of the treatments to identify the most effective remediation option.

Materials and Methods

Study area and water-sample collection

The study was conducted at Joseph Sarwuan Tarka University Makurdi (JOSTUM), Benue State, Nigeria, located at latitude 07°45.53′N and longitude 008°37.41′E. The university lies within the Southern Guinea Savanna agroecological zone and is characterized by an undulating terrain and seasonal streams that drain into the River Benue (Aguoru et al., 2014).

Water samples were collected from the university Waterworks, which supplies water for domestic and institutional use within the campus. The water was collected in ten clean containers, each with a capacity of 25 L, and transported to the Advanced Biology Laboratory, B41, JOSTUM, for contamination, treatment and laboratory analyses.

Collection and preparation of plant materials

Mature fruits containing *Moringa oleifera*, *Carica papaya* and *Citrus sinensis* seeds were purchased from Railway Market, Makurdi, Benue State. The plant materials were authenticated in the Department of Plant Science and Biotechnology, JOSTUM. Five kilograms of each seed type were separated from the fruits, washed with clean water and sun-dried. The dried seeds were pulverized using a mortar and pestle (Bichi, 2013). The resulting powders were stored in separate sterile, sealed bags and coded M, P and O for moringa, pawpaw and orange, respectively.

Green synthesis of magnesium oxide nanoparticles

Collection and preparation of *Jatropha tanjorensis* leaves

Fresh *Jatropha tanjorensis* leaves were collected from a farm in Tarka Local Government Area, Benue State, and authenticated in the Department of Plant Science and Biotechnology, JOSTUM. The leaves were washed with deionized water, air-dried and pulverized. Six grams of the powdered leaves were added to 100 mL of deionized water and heated at 80°C for 20–30 min. The extract was filtered through Whatman No. 1 filter paper and stored at 4°C until use (Essien et al., 2020).

Synthesis of MgONPs

Twenty millilitres of the prepared *Jatropha tanjorensis* leaf extract were transferred into a 250-mL beaker, stirred and heated to 60°C. Thereafter, 80 mL of a 0.2 M magnesium nitrate solution, prepared using 5 g of magnesium nitrate hexahydrate, were added dropwise. A few drops of 1 M sodium hydroxide were subsequently added, and the mixture was continuously stirred at 80°C for 4 h (Essien et al., 2020).

The formation of a yellowish-brown precipitate indicated the production of MgONPs. The mixture was centrifuged to separate the precipitate from the supernatant, after which the precipitate was washed repeatedly with 99.9% ethanol. The recovered material was oven-dried at

70°C for 3 h and calcined in a muffle furnace at 400°C for 2 h to obtain white MgONPs (Oyshi et al., 2025). The nanoparticles were stored in a Bijou bottle and coded N.

Characterization of green-synthesized magnesium oxide nanoparticles (MgONPs)

Ultraviolet-visible spectroscopy

The optical characteristics of the green-synthesized MgONPs were determined using a JENWAY 6405 UV-visible spectrophotometer. Absorbance was recorded over a wavelength range of 200-800 nm to confirm nanoparticle formation and determine the characteristic absorption peak (Essien et al., 2020).

Fourier-transform infrared spectroscopy

Fourier-transform infrared analysis was performed using an Agilent Cary 630 FTIR spectrometer. The MgONPs were prepared on potassium bromide discs using a 4% solid-to-KBr mixture. Spectra were recorded over the range of 400–4,000 cm^{-1} to identify the functional groups associated with nanoparticle formation and stabilization by compounds in the *Jatropha tanjorensis* extract (Essien et al., 2020).

Scanning electron microscopy

The morphology, surface structure, particle shape and aggregation of the MgONPs were examined using a Phenom World PRO:X 800-07334 scanning electron microscope, serial number MVE01570775. The micrographs were used to assess the surface characteristics and particle sizes of the synthesized material (Essien et al., 2020).

Energy-dispersive X-ray spectroscopy

Energy-dispersive X-ray spectroscopy coupled with the scanning electron microscope was used to determine the elemental composition of the synthesized nanoparticles. The elemental spectrum was examined to confirm the predominance of magnesium and oxygen and to identify other elements associated with residual plant-derived compounds.

X-ray diffraction

The crystalline properties of the MgONPs were examined using a Thermo Scientific ARL X'TRA X-ray diffractometer, serial number 197492086, at Umaru Musa Yar'adua University, Katsina State, Nigeria. The diffraction pattern was used to determine the crystalline phase, characteristic diffraction peaks and structural properties of the synthesized MgONPs (Essien et al., 2020).

Experimental design and treatments

The experiment was arranged in a completely randomized design with 15 remediation treatments and two controls; each replicated three times. This produced 51 experimental units. Each unit consisted of a labelled transparent plastic container containing 2.5 L of water, and the containers were randomized on the laboratory bench.

Powdered seed treatments were applied at 5 g per 2.5 L of contaminated water, equivalent to 2 g/L for each seed component, while MgONPs were applied at 200 mg/L. The positive control received Water Guard Plus containing sodium dichloroisocyanurate at the manufacturer's recommended rate of 5 g per 25 L, while the untreated control received no remediation material.

Treatment combinations and application rates

Code	Treatment components	Applied amount
M	Moringa seed powder	5 g/2.5 L
P	Pawpaw seed powder	5 g/2.5 L
O	Orange seed powder	5 g/2.5 L
N	MgONPs	200 mg/L
M+N	Moringa + MgONPs	5 g/2.5 L + 200 mg/L
M+O	Moringa + orange	5 g of each/2.5 L
M+P	Moringa + pawpaw	5 g of each/2.5 L
N+O	MgONPs + orange	200 mg/L + 5 g/2.5 L
N+P	MgONPs + pawpaw	200 mg/L + 5 g/2.5 L
P+O	Pawpaw + orange	5 g of each/2.5 L
M+N+O	Moringa + MgONPs + orange	5 g of each seed/2.5 L + 200 mg/L MgONPs
M+N+P	Moringa + MgONPs + pawpaw	5 g of each seed/2.5 L + 200 mg/L MgONPs
P+N+O	Pawpaw + MgONPs + orange	5 g of each seed/2.5 L + 200 mg/L MgONPs
P+M+O	Pawpaw + moringa + orange	5 g of each seed/2.5 L
M+P+N+O	Moringa + pawpaw + MgONPs + orange	5 g of each seed/2.5 L + 200 mg/L MgONPs
PC	WaterGuard Plus positive control	5 g/25 L
UC	Untreated contaminated-water control	No treatment

Water contamination and treatment procedure

Each experimental container was filled with 2.5 L of water and covered. The water was artificially contaminated with chemical compounds representing the physicochemical and heavy-metal contaminants investigated in the study. The compounds included calcium carbonate, magnesium sulphate, silver nitrate, copper sulphate, lead nitrate, sodium chloride, potassium iodide, phosphorus trichloride, nickel acetate and mercury chloride. Five grams of each contaminating compound were introduced into the respective experimental containers, and the containers were tightly covered and sealed with masking tape (Hadi et al., 2014).

The contaminated water was maintained under laboratory conditions before baseline assessment. Baseline measurements included pH, total dissolved solids, total suspended solids, electrical conductivity, hardness, biochemical oxygen demand, nitrate, sulphate, phosphate and the concentrations of Cd, Ni, Pb, Hg and Ag.

Following baseline assessment, the individual and combined treatments were applied at their designated concentrations. The treatment experiment was monitored from week 2 to week 10, with water-quality assessments conducted at two-week intervals (Hadi et al., 2014).

Physicochemical analyses

The pH, electrical conductivity and total dissolved solids were determined using a HANNA HI 98129 multiparameter water tester. The probe was immersed in each water sample, and the appropriate measurement mode was selected. Electrical conductivity was expressed as µS/cm, while total dissolved solids were expressed as mg/L (AOAC, 2012).

Total suspended solids were determined using standard procedures described by AOAC (2012). Total hardness was measured using the Palintest Hardicol colorimetric method. Hardicol reagent tablets were added to the water samples, allowing calcium and magnesium ions to produce a purple colour whose intensity was measured using a Palintest photometer. Total hardness was expressed as mg/L $CaCO_3$ (AOAC, 2012).

Biochemical oxygen demand was determined from the difference between dissolved oxygen concentrations measured before and after incubation (AOAC, 2012):

$$\mathbf{BOD(mg/L) = DO_{\text{before incubation}} - DO_{\text{after incubation}}}$$

Determination of nitrate, sulphate and phosphate

Nitrate, sulphate and phosphate concentrations were determined using a Lovibond Tintometer MD 600. The appropriate parameter was selected; the prepared sample was inserted into the instrument and the concentration displayed on the screen was recorded in mg/L (AOAC, 2012).

For the sulphate turbidity test, 10 mL of each sample were transferred into a test tube, after which one Sulphate Turb tablet was added, crushed and mixed until dissolved. The sample was allowed to stand for 5 min, and sulphate concentration was measured using a Palintest photometer and expressed as mg/L SO_4^{2-} (AOAC, 2012).

Heavy-metal analysis

Standard stock solutions were prepared separately for Cd, Ni, Pb, Hg and Ag by dissolving appropriate quantities of the respective metals or their salts. The solutions were stored in plastic containers to minimize possible metal leaching from glassware. Water samples were digested according to AOAC (2012) procedures before instrumental determination.

The concentrations of Cd, Ni, Pb, Hg and Ag were measured using an atomic absorption spectrophotometer fitted with the appropriate lamp for each element (Ali et al., 2013). Each sample was analyzed in triplicate, and metal concentrations were expressed in parts per million. Triplicate determinations, reagent blanks, standard solutions and instrument calibration were used to maintain analytical quality.

Calculation of heavy-metal removal efficiency

The removal efficiency of each treatment was calculated as:

$$\mathbf{[(C_0 - C_t)/C_0] \times 100}.$$

where C_0 represents the initial metal concentration in the contaminated water before treatment and C_t represents the concentration after treatment.

Estimation of Pollution Indices

The contamination factor for each metal (CF_i) was calculated by dividing its measured concentration (C_i) by the corresponding reference concentration (S_i): $CF_i = C_i/S_i$. The integrated pollution load index (I-PLI) was calculated as the mean of the five contamination factors: I-PLI = $\Sigma CF_i/n$, where n = 5 (Kowalska et al., 2018).

The Heavy Metal Pollution Index (HPI) was subsequently calculated as HPI = I-PLI/10. The reference concentrations used were 0.003 ppm for Cd, 0.07 ppm for Ni, 0.01 ppm for Pb, 0.006 ppm for Hg and 0.1 ppm for Ag (WHO, 2022; Joanna *et al.,* 2018).

Statistical analysis

Data were analyzed using Minitab version 17.0. Results from the three replicates were summarized using means and standard deviations. Analysis of variance was used to determine significant differences among treatment means, and Fisher's Least Significant Difference test was used for mean separation at $p \leq 0.05$. For multivariate analysis, physicochemical and heavy-metal variables were standardized to remove scale effects, and hierarchical cluster analysis was performed using Euclidean distance and Ward's linkage. Only treatments with complete observations for both physicochemical properties and heavy-metal concentrations were included; the positive control and treatments with incomplete physicochemical records were excluded from the integrated clustering.

Results

Characterization of green-synthesized MgONPs

UV–visible characteristics

The UV-Visible absorption spectra of the *Jatropha tanjorensis* leaf extract and the synthesized MgONPs showed a prominent absorption peak at approximately 280 nm. The observed absorption peak supported the formation of MgONPs.

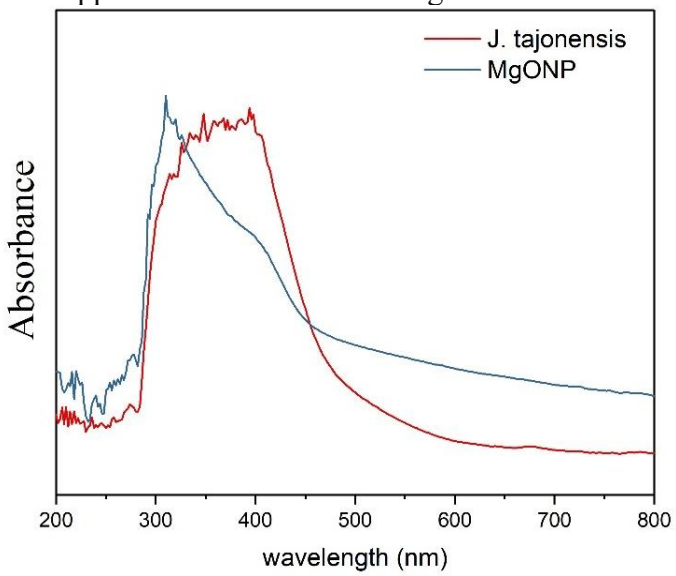


Figure 1: UV-VIS Spectra of *Jatropha tanjorensis* Leaf Extract and Magnesium Oxide Nanoparticles

Fourier-transform infrared characteristics

The FTIR spectrum showed a broad absorption band around 3400 cm^{-1}, corresponding to O-H stretching vibrations associated with hydroxyl-containing compounds. A prominent band at approximately 1000 cm^{-1} was assigned to Mg-O stretching vibrations, confirming the formation of magnesium oxide. Additional bands between 800 and 500 cm^{-1} were attributed to the bending vibrations of Mg-O bonds.

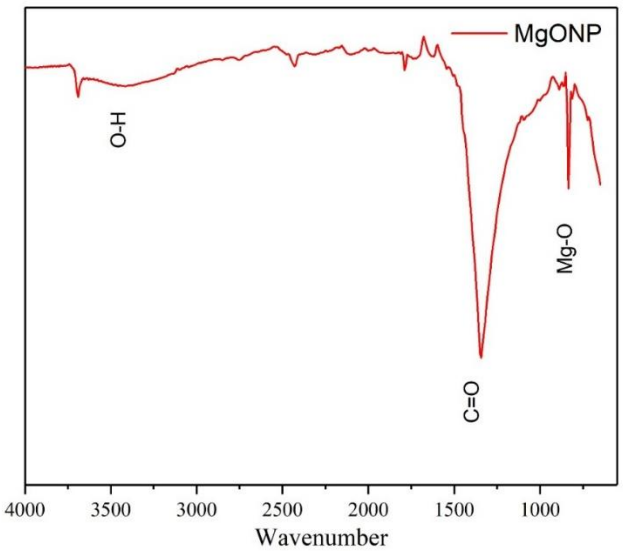


Figure 2: FTIR Spectrum of the synthesized Magnesium Oxide Nanoparticles

SEM morphology

The SEM analysis showed that the MgONPs possessed a relatively uniform spherical morphology. The particle surfaces appeared smooth, with no substantial agglomeration. The observed particles were within the nanometre size range.

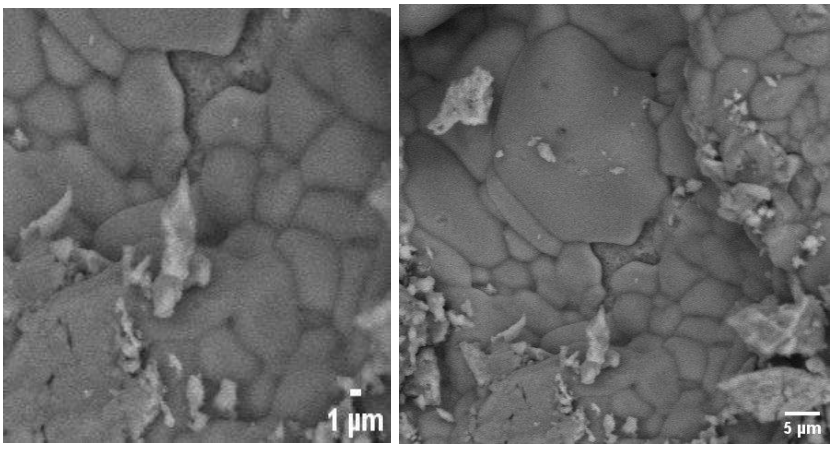


Plate 1: SEM Images of the Synthesized Magnesium Oxide Nanoparticles

EDX elemental composition

The EDX analysis showed that magnesium was the predominant element in the synthesized nanoparticles. The recorded atomic and weight concentrations of magnesium were 46.51% and 46.46%, respectively, confirming the presence of magnesium in the synthesized material.

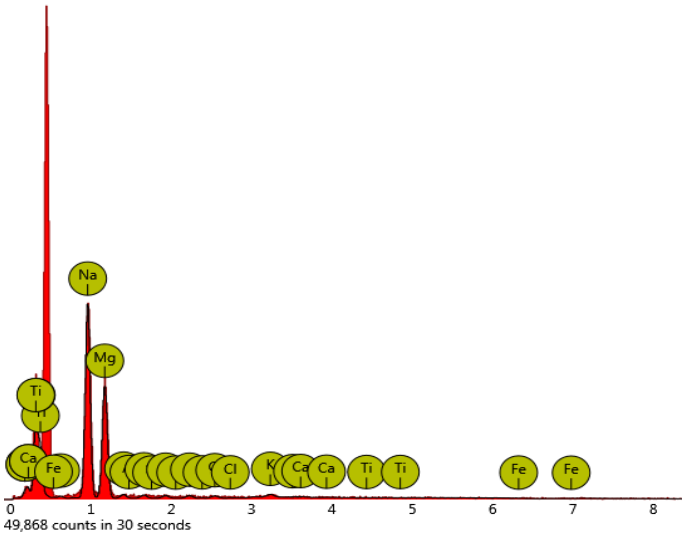


Figure 3: EDX Spectra of the Magnesium Oxide Nanoparticles

XRD crystalline structure

The XRD pattern showed diffraction peaks between 8.64° and 67.31°, corresponding to the different crystallographic planes of MgONPs. The average crystallite size was 22.33 nm, confirming the nanoscale and crystalline nature of the synthesized MgO material.

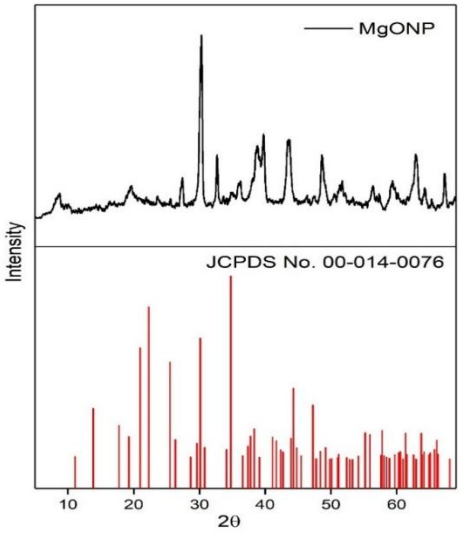


Figure 4: XRD Pattern of Magnesium Oxide Nanoparticles Derived from *Jatropha tajorensis*

Effects of treatments on physicochemical properties

The single and combined treatments significantly affected all the physicochemical properties of the contaminated water (Table 1). The pH values ranged from 7.08 in the untreated control to 7.92 in the MgONP treatment. Although the treatments produced statistically significant differences in pH, all the recorded values remained slightly neutral to alkaline.

The untreated control recorded TDS and TSS values of 100.30 and 77.70 mg/L, respectively. All seed-powder and nanoparticle treatments increased these parameters. The M+P+N+O treatment recorded the highest TDS (545.33 mg/L), TSS (620.00 mg/L) and electrical conductivity (987.67 µS/cm), whereas the untreated control recorded the lowest values of 100.30 mg/L, 77.70 mg/L and 212.00 µS/cm, respectively.

Total hardness ranged from 42.33 mg/L in the positive control to 357.33 mg/L in the M+P+N+O treatment. Among the remediation treatments, P+N+O recorded the lowest hardness (148.67 mg/L). Only P, M and N produced BOD values below that of the untreated control (68.33 mg/L). M recorded the lowest BOD among the remediation treatments (62.67 mg/L), whereas M+P+N+O recorded the highest value (266.33 mg/L).

The treatments did not produce uniform improvements in the physicochemical properties of the water. Some treatments reduced BOD, but most seed and nanoparticle treatments increased TDS, TSS, electrical conductivity and hardness relative to the untreated control.

© IIJP 2026 | Volume 2, Issue 3, pp. 2005-2025 | ISSN: 2636-4484

Table 1. Effects of individual and combined treatments on the physicochemical properties of heavy metal-contaminated water

Treatments	pH	TDS (mg/L)	TSS (mg/L)	EC (µS/cm)	Hardness (mg/L)	BOD (mg/L)
O	7.85 ± 0.00^{b}	196.30 ± 1.50^{j}	264.00 ± 1.00^{i}	394.70 ± 3.10^{h}	155.67 ± 2.08^{ef}	87.00 ± 2.65^{i}
P	7.72 ± 0.01^{c}	167.30 ± 1.20^{k}	185.00 ± 2.00^{j}	232.00 ± 0.00^{j}	154.33 ± 2.08^{fg}	63.67 ± 1.16^{jk}
M	7.70 ± 0.03^{c}	165.30 ± 1.20^{k}	178.00 ± 3.60^{j}	242.00 ± 1.70^{i}	165.00 ± 1.73^{d}	62.67 ± 2.89^{k}
N	7.92 ± 0.01^{a}	166.70 ± 1.20^{k}	184.30 ± 3.10^{j}	236.00 ± 6.90^{ij}	157.67 ± 7.37^{ef}	64.67 ± 1.53^{jk}
M+N	7.82 ± 0.00^{b}	210.00 ± 1.00^{i}	318.70 ± 1.50^{g}	413.00 ± 2.00^{g}	161.00 ± 0.00^{de}	94.67 ± 2.31^{h}
M+O	7.54 ± 0.01^{e}	294.33 ± 4.73^{e}	379.33 ± 14.01^{d}	562.00 ± 13.75^{c}	273.67 ± 4.16^{c}	184.33 ± 2.52^{e}
M+P	7.22 ± 0.01^{f}	316.33 ± 5.03^{c}	386.00 ± 3.61^{d}	454.00 ± 7.94^{e}	340.67 ± 8.50^{b}	126.33 ± 5.69^{g}
N+O	7.16 ± 0.01^{hi}	378.00 ± 2.00^{b}	477.00 ± 2.00^{b}	539.33 ± 7.37^{d}	353.00 ± 3.00^{a}	163.67 ± 3.51^{f}
N+P	7.13 ± 0.04^{ij}	310.70 ± 1.20^{d}	419.00 ± 2.70^{c}	645.30 ± 1.20^{b}	166.33 ± 0.58^{d}	165.67 ± 0.58^{f}
M+N+P	7.12 ± 0.01^{j}	277.70 ± 0.60^{f}	356.00 ± 0.00^{e}	539.30 ± 1.20^{d}	152.67 ± 0.58^{fg}	189.33 ± 1.53^{d}
P+N+O	7.17 ± 0.01^{gh}	231.70 ± 1.20^{h}	298.30 ± 1.50^{h}	456.00 ± 0.00^{e}	148.67 ± 2.08^{g}	212.33 ± 1.16^{c}
P+M+O	7.15 ± 0.00^{hij}	246.00 ± 1.00^{g}	343.70 ± 1.20^{f}	431.70 ± 1.20^{f}	165.67 ± 0.58^{d}	223.00 ± 3.00^{b}
M+P+N+O	7.20 ± 0.01^{fg}	545.33 ± 3.51^{a}	620.00 ± 1.00^{a}	987.67 ± 6.03^{a}	357.33 ± 4.04^{a}	266.33 ± 4.73^{a}
Positive control	7.59 ± 0.02^{d}	109.00 ± 2.00^{l}	98.30 ± 2.30^{k}	431.30 ± 2.90^{f}	42.33 ± 3.79^{i}	65.33 ± 1.16^{jk}
Untreated control	7.08 ± 0.04^{k}	100.30 ± 2.90^{m}	77.70 ± 3.50^{l}	212.00 ± 0.00^{k}	128.00 ± 6.24^{h}	68.33 ± 2.52^{j}
F-value	841.40	6646.79	3529.42	4244.17	1594.36	1808.12
p-value	<0.001	<0.001	<0.001	<0.001	<0.001	<0.001

Note. O = orange; P = pawpaw; M = moringa; N = MgONPs. P+O and M+N+O are not presented because their physicochemical measurements were unavailable.

TDS = total dissolved solids; TSS = total suspended solids; EC = electrical conductivity; BOD = biochemical oxygen demand. Values are means ± SD (n = 3). Within each column, means sharing a superscript letter are not significantly different according to Fisher's LSD test ($p > 0.05$).

Effects of treatments on nitrate, sulphate and phosphate

The treatments significantly affected nitrate ($F = 262.38$, $p < 0.001$) and phosphate concentrations ($F = 263.00$, $p < 0.001$), whereas their effects on sulphate were not significant ($F = 1.54$, $p = 0.156$; Table 2). The untreated control recorded the lowest nitrate concentration (0.11 mg/L), followed by the positive control (0.20 mg/L). Among the seed-powder and nanoparticle

treatments, M and N+O produced the lowest nitrate concentration (0.37 mg/L), whereas N+P recorded the highest concentration (1.11 mg/L).

Sulphate concentrations ranged from 0.13 to 0.77 mg/L among the treatments. M, N+O and the positive control recorded the lowest value of 0.13 mg/L, while N+P produced the highest sulphate concentration of 0.77 mg/L. However, these differences were not statistically significant.

Phosphate concentration was lowest in the untreated control at 1.03 mg/L and the positive control at 1.07 mg/L. Among the remediation treatments, M and N+O produced the lowest phosphate concentration of 2.23 mg/L, whereas N+P produced the highest concentration of 3.17 mg/L. These results showed that the application of the seed materials and MgONPs generally increased nitrate and phosphate concentrations relative to the untreated water.

Table 2. Effects of individual and combined treatments on nutrient concentrations in heavy metal-contaminated water

Treatments	Nitrate (mg/L)	Sulphate (mg/L)	Phosphate (mg/L)
O	0.87 ±0.02^{c}	0.40 ±0.00	2.40 ±0.00^{e}
P	0.43 ±0.06^{d}	0.20 ±0.00	2.43 ±0.06d^{e}
M	0.37 ±0.06^{e}	0.13 ±0.06	2.23 ±0.06^{f}
N	0.43 ±0.06^{d}	0.20 ±0.00	2.33 ±0.12e^{f}
M+N	0.92 ±0.01^{bc}	0.47 ±0.06	2.53 ±0.06d
M+O	0.87 ±0.02^{c}	0.40 ±0.00	2.40 ±0.00e
M+P	0.43 ±0.06^{d}	0.20 ±0.00	2.43 ±0.06de
N+O	0.37 ±0.06^{e}	0.13 ±0.06	2.23 ±0.06^{f}
N+P	1.11 ±0.01^{a}	0.77 ±0.06	3.17 ±0.06^{a}
M+N+P	0.90 ±0.01^{bc}	0.67 ±0.06	2.83 ±0.06^{b}
P+N+O	0.88 ±0.01^{c}	0.50 ±0.00	2.70 ±0.00^{c}
P+M+O	0.95 ±0.01^{b}	0.40 ±0.12	2.70 ±0.00^{c}
M+P+N+O	0.92 ±0.01^{bc}	0.47 ±0.06	2.53 ±0.06^{d}
Positive control	0.20 ±0.02^{f}	0.13 ±0.06	1.07 ±0.06^{g}
Negative control	0.11 ±0.00^{g}	0.27 ±0.06	1.03 ±0.12^{g}
F-value	262.38	1.54	263.0
p-value	<0.001	0.156	<0.001

Note. O = orange; P = pawpaw; M = moringa; N = MgONPs. P+O and M+N+O are not presented because their nutrient measurements were unavailable. Values are means ± SD (n = 3).

© IIJP 2026 | Volume 2, Issue 3, pp. 2005-2025 | ISSN: 2636-4484

Effects of treatments on heavy-metal concentrations

The untreated contaminated water contained 1.381 ppm Cd, 1.984 ppm Ni, 1.585 ppm Pb, 1.184 ppm Hg and 1.266 ppm Ag. All the treatments significantly affected the concentrations of the five heavy metals (Table 3).

Cadmium

Cadmium concentration decreased from 1.381 ppm in the untreated control to 0.024 ppm in the P+O treatment, representing a removal efficiency of 98.26%. The M+N and P treatments also reduced Cd to 0.025 and 0.033 ppm, respectively. The highest residual Cd concentration among the treated samples was recorded in M+P+N+O at 0.350 ppm. Thus, P+O was the most effective treatment for Cd removal.

Nickel

Nickel concentration was reduced most effectively by N+P, which decreased the concentration from 1.984 to 0.033 ppm, corresponding to 98.34% removal. The M+P and P+O treatments also produced low residual Ni concentrations of 0.078 and 0.087 ppm, respectively. In contrast, M+N+P recorded the highest residual Ni concentration of 1.723 ppm.

Lead

Lead concentration decreased from 1.585 ppm in the untreated control to an undetectable concentration of 0.000 ppm in the P+O and M+P+N+O treatments, representing 100% removal. The N+P treatment produced the next lowest Pb concentration of 0.012 ppm, followed by M+P at 0.029 ppm and M+N+O at 0.035 ppm. Pawpaw–orange was therefore among the most effective treatments for Pb removal.

Mercury

The lowest residual Hg concentration was recorded in P+O at 0.007 ppm, representing a reduction of 99.41% relative to the untreated control. This was followed by M+N+O and M+P, which reduced Hg to 0.016 and 0.017 ppm, respectively. The M+P+N+O treatment recorded the highest residual Hg concentration among the treated samples at 0.132 ppm.

Silver

Silver concentration decreased from 1.266 ppm in the untreated control to an undetectable concentration of 0.000 ppm under several treatments. These included O, P, M, M+N, N+O, N+P, P+O and M+N+P, corresponding to 100% removal. Among the treatments with detectable Ag concentrations, N produced the lowest value of 0.002 ppm, followed by M+O at 0.005 ppm.

Table 3. Effects of individual and combined treatments on heavy-metal concentrations in contaminated water

Treatments	Cadmium (ppm)	Nickel (ppm)	Lead (ppm)	Mercury (ppm)	Silver (ppm)
O	0.065^{k} ±0.000	0.813^{e} ±0.001	0.074^{h} ±0.001	0.047^{f} ±0.000	0.000^{i} ±0.000
P	0.033^{m} ±0.000	0.782^{f} ±0.001	0.068^{i} ±0.000	0.035^{h} ±0.000	0.000^{i} ±0.000
M	0.083^{h} ±0.000	0.265^{k} ±0.000	0.121^{g} ±0.000	0.036^{h} ±0.000	0.000^{i} ±0.000
N	0.065^{k} ±0.000	0.454^{i} ±0.001	0.183^{e} ±0.001	0.074^{c} ±0.000	0.002^{h} ±0.000
M+N	0.025^{n} ±0.000	0.366^{j} ±0.003	0.076^{h} ±0.002	0.062^{d} ±0.000	0.000^{i} ±0.000
M+O	0.138^{f} ±0.000	0.652^{h} ±0.001	0.216^{d} ±0.001	0.057^{e} ±0.000	0.005^{g} ±0.000
M+P	0.039^{l} ±0.000	0.078^{n} ±0.001	0.029^{l} ±0.001	0.017^{k} ±0.000	0.018^{e} ±0.000
N+O	0.258^{d} ±0.000	1.535^{c} ±0.002	0.062^{j} ±0.002	0.023^{j} ±0.000	0.000^{i} ±0.000
N+P	0.156^{e} ±0.000	0.033^{o} ±0.001	0.012^{m} ±0.000	0.038^{g} ±0.000	0.000^{i} ±0.000
P+O	0.024^{o} ±0.000	0.087^{m} ±0.001	0.000^{n} ±0.000	0.007^{m} ±0.000	0.000^{i} ±0.000
M+N+P	0.092^{g} ±0.000	1.723^{b} ±0.001	0.165^{f} ±0.001	0.038^{g} ±0.000	0.000^{i} ±0.000
M+N+O	0.079^{i} ±0.000	0.255^{l} ±0.002	0.035^{k} ±0.001	0.016^{l} ±0.000	0.052^{b} ±0.000
P+N+O	0.074^{j} ±0.000	0.653^{h} ±0.001	0.323^{b} ±0.002	0.057^{e} ±0.000	0.022^{d} ±0.000
P+M+O	0.335^{c} ±0.000	0.676g ±0.006	0.265^{c} ±0.001	0.033i ±0.000	0.028^{c} ±0.000
M+P+N+O	0.350^{b} ±0.000	0.823^{d} ±0.001	0.000^{n} ±0.000	0.132^{b} ±0.001	0.013^{f} ±0.000
Untreated control	1.381^{a} ±0.001	1.984^{a} ±0.004	1.585^{a} ±0.003	1.184^{a} ±0.002	1.266^{a} ±0.001
F-value	246.51	188.23	263.57	697.26	223.22
p-value	<0.001	<0.001	<0.001	<0.001	<0.001

Note. O = orange; P = pawpaw; M = moringa; N = MgONPs. Values are means ± SD (n = The positive control is not presented because its heavy-metal measurements were unavailable.

Comparative treatment performance

The effectiveness of the treatments varied according to the heavy metal considered. Pawpaw-orange produced the lowest residual concentrations of Cd, Pb and Hg and completely removed Ag. It reduced Cd, Pb, Hg and Ag by 98.26%, 100%, 99.41% and 100%, respectively. However, N+P was more effective against Ni, producing 98.34% removal compared with 95.61% under P+O. Therefore, P+O demonstrated the best broad-spectrum heavy-metal remediation, while N+P showed greater metal-specific effectiveness against Ni.

Heavy Metal Pollution Index

The HPI values varied considerably among treatments (Table 4). The untreated contaminated water recorded the highest HPI of 17.150. Among the single treatments, P produced the lowest HPI of 0.700, followed by O at 0.975 and M at 0.987, whereas N recorded an HPI of 1.181 and was classified as not remediated.

Among the combined treatments, P+O produced the lowest HPI (0.211), followed by M+P (0.404), M+N (0.632) and M+N+O (0.738). N+O recorded an HPI of 2.359 and was

classified as not remediated. M+O, N+P, N+O, M+N+P, P+N+O, P+M+O and M+P+N+O all recorded HPI values above 1.0. Overall, P+O was the most effective treatment for reducing the cumulative heavy-metal burden.

Table 4. Heavy Metal Pollution Index of water subjected to individual and combined treatments

Treatment	Code	HPI	Interpretation
Orange seed	O	0.975	Remediated
Pawpaw seed	P	0.700	Remediated
Moringa seed	M	0.987	Remediated
MgONPs	N	1.181	Not remediated
Moringa + MgONPs	M+N	0.632	Remediated
Moringa + orange	M+O	1.729	Not remediated
Moringa + pawpaw	M+P	0.404	Remediated
MgONPs + orange	N+O	2.359	Not remediated
Pawpaw + MgONPs	N+P	1.203	Not remediated
Pawpaw + orange	P+O	0.211	Remediated
Moringa + orange + MgONPs	M+N+O	0.738	Remediated
Moringa + pawpaw + MgONPs	M+N+P	1.566	Not remediated
Pawpaw + orange + MgONPs	P+N+O	1.515	Not remediated
Pawpaw + moringa + orange	P+M+O	3.076	Not remediated
Moringa + pawpaw + orange + MgONPs	M+P+N+O	3.008	Not remediated
Untreated contaminated water	UC	17.150	Not remediated

HPI < 1.0 = remediated; HPI ≥ 1.0 = not remediated.

Cluster analysis of treatment effects

Hierarchical cluster analysis of treatments with complete physicochemical and heavy-metal records produced four interpretable groups. The individual seed powders and MgONPs (O, P, M and N), together with M+N, formed a low-to-moderate physicochemical-response cluster. M+O, M+P, N+O, N+P, M+N+P, P+N+O and P+M+O formed a second cluster characterized generally by greater changes in dissolved or suspended constituents and treatment-specific residual metal concentrations. The complete M+P+N+O treatment formed a separate cluster because of its markedly high TDS, TSS, EC, hardness and BOD, while the untreated control was isolated because of its substantially higher overall heavy-metal burden. The positive control, P+O and M+N+O were excluded from this integrated analysis because complete measurements across both variable sets were unavailable. These groupings indicate that increasing treatment complexity altered the overall water-quality profile but did not consistently improve heavy-metal remediation.

Discussion

The UV–Visible absorption peak at approximately 280 nm, together with the FTIR bands assigned to O–H and Mg–O vibrations, supported the formation of plant-mediated MgONPs. The XRD-derived average crystallite size of 22.33 nm further confirmed the nanoscale crystalline structure, while the predominantly spherical SEM morphology and magnesium-rich EDX spectrum supported the identity of the synthesized material. Plant metabolites associated with the particle surface may have acted as stabilizing or capping agents and may also have supplied additional hydroxyl and other oxygen-containing sites for metal binding, as reported for green-synthesized MgONPs (Rotti et al., 2023).

Treatment pH remained within a near-neutral to mildly alkaline range of 7.08–7.92. Under these conditions, reduced competition from hydrogen ions can promote deprotonation of hydroxyl and carboxyl groups on plant materials, increasing their attraction for positively charged metal ions. Near-neutral conditions may also support metal-hydroxide formation; consequently, the observed reductions probably reflected a combination of adsorption, coagulation and partial precipitation rather than adsorption alone. Moringa proteins can additionally destabilize charged particles and promote floc formation (Camacho et al., 2017).

The treatments did not uniformly improve the general physicochemical quality of the water. The complete M+P+N+O treatment produced the highest TDS, TSS, EC, hardness and BOD, and several other combinations also exceeded the untreated control. These increases may have resulted from soluble ions, fine particles, proteins, oils and carbohydrates released from the seed powders, together with magnesium-containing species contributed by MgONPs. The accompanying elevation of BOD is particularly important because biodegradable seed constituents can increase microbial oxygen demand. Thus, effective metal removal did not necessarily produce water suitable for direct consumption, and sedimentation or filtration would be required to remove residual biomass and nanoparticles.

Nitrate and phosphate generally increased after treatment, whereas sulphate did not differ significantly among treatments. Nutrient enrichment was greatest under N+P, while the untreated and positive controls generally recorded lower concentrations. The seed powders may have released nitrogen- and phosphorus-containing organic compounds or minerals during contact with water. This secondary enrichment reinforces the need to optimize treatment dose and contact time because excess residual nutrients may encourage microbial growth or eutrophication if treated water is discharged without polishing.

All treatments reduced Cd, Ni, Pb, Hg and Ag relative to the untreated control, but effectiveness was metal- and treatment-specific. Plant-derived biosorbents contain hydroxyl, carboxyl, carbonyl, amino and amide groups that can bind metals through ion exchange, electrostatic attraction, chelation and surface complexation (Hegazy et al., 2021). MgONPs provide additional reactive inorganic surfaces on which adsorption, complexation and precipitation may occur (Ghoniem et al., 2022). Differences in ionic radius, hydration energy, speciation and affinity for particular functional groups may therefore explain why no treatment performed uniformly across all metals.

P+O showed the strongest broad-spectrum performance, producing the lowest residual Cd and Hg, complete Pb and Ag removal and the lowest HPI. Pawpaw seed surfaces contain functional groups capable of binding metal ions, while orange seed biomass provides a lignocellulosic matrix with additional adsorption sites. The performance of orange-seed-derived material in contaminant adsorption has also been demonstrated in real wastewater (Flores Alarcón

et al., 2022). The combined availability of chemically different binding sites may therefore have improved the range of metals retained by P+O.

In contrast, N+P was the most effective treatment for Ni, reducing its concentration by 98.34%, but its HPI remained above the remediation threshold because the index reflected the combined contributions of all five metals. This distinction shows why removal of one target metal cannot be used as evidence of overall remediation. Similarly, N+O completely removed Ag and retained low residual Pb and Hg, yet its HPI of 2.359 was driven principally by comparatively high residual Cd and Ni. The inclusion of N+O therefore strengthens the conclusion that treatment performance must be assessed across the entire contaminant mixture.

Not all combinations outperformed the individual materials. Organic matter may coat MgONP surfaces, nanoparticles may aggregate, and dissolved metals may compete for the same binding sites, thereby reducing the number of accessible reactive sites. Accordingly, the results support treatment-specific complementary effects but do not demonstrate universal synergy. Establishing synergy would require a factorial interaction analysis showing that a combined response exceeded the response expected from its individual components.

The cluster analysis showed that the individual materials and M+N clustered together because their overall physicochemical disturbances were generally lower, whereas most multi-material treatments formed a broader cluster with larger changes in water-quality variables and variable residual-metal profiles. M+P+N+O separated from the other treatments because of its pronounced physicochemical loading, while the untreated control separated because of its high metal concentrations. The clustering therefore indicates that adding more treatment components changed the water-quality profile without guaranteeing better cumulative remediation.

The findings demonstrate a trade-off between heavy-metal removal and secondary water-quality changes. P+O offered the most favourable cumulative metal reduction, while N+P provided the strongest Ni-specific performance. However, increases in dissolved solids, suspended solids, hardness, nutrients and BOD under several combinations show that the materials should be regarded as preliminary remediation agents rather than complete drinking-water treatments. Practical application will require dosage optimization, separation of spent adsorbents, assessment of residual nanoparticles and post-treatment polishing before treated water can be considered safe.

Conclusion

This study provides comparative evidence on the individual and combined application of moringa, pawpaw and orange seed powders and green-synthesized MgONPs for treating multi-metal-contaminated water, integrating conventional physicochemical measurements, metal-removal efficiencies and HPI within a single experiment. The synthesized MgONPs exhibited spectral characteristics consistent with MgO formation, while the treatments produced varying reductions in Cd, Ni, Pb, Hg and Ag. Pawpaw combined with MgONPs showed particularly strong nickel-removal performance, whereas the pawpaw–orange treatment produced the lowest HPI and therefore the most favourable overall reduction in heavy-metal pollution. However, several combined treatments increased TDS, TSS, EC, hardness and BOD, demonstrating that improved metal removal does not automatically correspond to acceptable overall water quality. The findings establish that treatment performance is determined by the specific interaction between the adsorbent materials and individual metal ions rather than simply by increasing the number of treatment components. Seed powders and MgONPs therefore offer promising preliminary remediation options, but dosage optimization, material recovery and post-treatment polishing are necessary before practical drinking-water application.

Recommendations

The pawpaw–orange and pawpaw–MgONP treatments should be prioritized for further optimization because of their respective HPI and nickel-removal performance. Further experiments should evaluate treatment dosage, contact time, adsorption kinetics, equilibrium behaviour, regeneration, residual nanoparticles and possible toxicity. The treatments should also be tested using larger sample sizes and under field conditions to determine their effectiveness in naturally variable water systems.

JOSTUM Waterworks and other local water managers should not apply the tested combinations directly to drinking-water production at this stage. Any pilot application should include controlled dosing, sedimentation or filtration, residual nanoparticle monitoring, microbial analysis and confirmation that all treated-water parameters meet applicable drinking-water standards before distribution or consumption.

Declarations

Acknowledgements

The authors acknowledge the laboratory and technical support provided by Joseph Sarwuan Tarka University Makurdi and Umaru Musa Yar'adua University, Katsina State.

Conflict of interest

The authors declare that they have no competing interests.

Data-availability statement

The data supporting the findings of this study are available from the corresponding author upon reasonable request.

Ethical and environmental compliance

The study did not involve human participants or experimental animals. Laboratory procedures were conducted in accordance with applicable institutional safety and environmental requirements.

References

Adekitan, A. A., Oyewumi, J. O., Dada, V. O., Layi-Adigun, B. O., & Raheem, I. (2023). Use of neem leaf, pawpaw seed and moringa seed as natural coagulants for surface water treatment. *Journal of Applied Sciences and Environmental Management, 27*(7), 1347–1352.

Aguoru, C. U., Uduaga, B. E., & Olasan, J. O. (2014). Ecological pattern and distribution of economic trees in the Federal University of Agriculture, Makurdi, North Central Guinea Savannah, Nigeria. *International Journal of Tropical Agriculture and Food Systems, 8*(1), 10–11.

Ali, H., Khan, E., & Sajad, M. A. (2013). Phytoremediation of heavy metals—Concepts and applications. *Chemosphere, 91*(7), 869–881.

Amran, A. H., Zaidi, N. S., Muda, K., Bahrodin, M. B., & Loan, L. W. (2021). Deshelled *Carica papaya* seeds as a natural coagulant for improving river-water quality. *Sains Malaysiana, 50*(6), 1521–1529.

AOAC International. (2012). *Official methods of analysis of AOAC International* (19th ed.; G. W. Latimer Jr., Ed.). AOAC International.

Aziz, N. A. A., Jayasuriya, N., & Fan, L. (2016). Adsorption study on *Moringa oleifera* seeds and *Musa cavendish* as natural water-purification agents for the removal of lead, nickel and cadmium from drinking water. *IOP Conference Series: Materials Science and Engineering, 136*, 012044.

Barakat, M. A. (2011). New trends in removing heavy metals from industrial wastewater. *Arabian Journal of Chemistry, 4*(4), 361–377.

Bichi, M. H. (2013). A review of the applications of *Moringa oleifera* seed extract in water treatment. *Civil and Environmental Research, 3*(8), 1–10.

Cai, Y., Li, C., Wu, D., Wang, W., Tan, F., Wang, X., Wong, P. K., & Qiao, X. (2017). Highly active MgO nanoparticles for simultaneous bacterial inactivation and heavy-metal removal from aqueous solution. *Chemical Engineering Journal, 312*, 158–166.

Camacho, F. P., Sousa, V. S., Bergamasco, R., & Teixeira, M. R. (2017). The use of *Moringa oleifera* as a natural coagulant in surface-water treatment. *Chemical Engineering Journal, 313*, 226–237.

Essien, E. R., Atasie, V. N., Okeafor, A. O., & Nwude, D. O. (2020). Biogenic synthesis of magnesium oxide nanoparticles using *Manihot esculenta* (Crantz) leaf extract. *International Nano Letters, 10*, 43–48.

Flores Alarcón, M. A. D., Revilla Pacheco, C., Garcia Bustos, K., Tejada Meza, K., Terán-Hilares, F., Pacheco Tanaka, D. A., Colina Andrade, G. J., & Terán-Hilares, R. (2022). Efficient dye

removal from real textile wastewater using orange-seed powder as a suitable bioadsorbent and membrane technology. *Water, 14*(24), 4104.

Genchi, G., Carocci, A., Lauria, G., Sinicropi, M. S., & Catalano, M. (2020). Nickel: Human health and environmental toxicology. *International Journal of Environmental Research and Public Health, 17*(3), 679.

Ghoniem, M. G., Ben Aissa, M. A., Ali, F. A. M., & Khairy, M. (2022). Efficient and rapid removal of Pb(II) and Cu(II) heavy metals from aqueous solutions by MgO nanorods. *Inorganics, 10*(12), 256.

Hadi, F., Ali, N., & Ahmad, A. (2014). Enhanced phytoremediation of cadmium-contaminated soil by *Parthenium hysterophorus*: Effect of gibberellic acid and synthetic chelator, alone and in combinations. *Bioremediation Journal, 18*(1), 46–55.

Hasan, H. A., Muhammad, M. H., & Ismail, N. (2020). A review of biological drinking-water treatment technologies for contaminant removal from polluted water resources. *Journal of Water Process Engineering, 33*, 101035.

He, Y., Ingudam, S., Reed, S., Gehring, A., Strobaugh, T. P., Jr., & Irwin, P. (2016). Study on the mechanism of antibacterial action of magnesium oxide nanoparticles against foodborne pathogens. *Journal of Nanobiotechnology, 14*, 54.

Hegazy, I., Ali, M. E. A., Zaghlool, E. H., & Elsheikh, R. (2021). Heavy-metal adsorption from contaminated water using moringa seeds/olive-pomace by-products. *Applied Water Science, 11*, 95.

Jaishankar, M., Tseten, T., Anbalagan, N., Mathew, B. B., & Beeregowda, K. N. (2014). Toxicity, mechanism and health effects of some heavy metals. *Interdisciplinary Toxicology, 7*(2), 60–72.

Joanna, B. K., Ryszard, M., Michal, G. and Tomasz, Z. (2018). Pollution indices as useful tools for a comprehensive evaluation of the degree of soil contamination – A review. *Environment, Geochemical and Health*. 40: 2395-2420.

Kowalska, J. B., Mazurek, R., Gąsiorek, M., & Zaleski, T. (2018). Pollution indices as useful tools for the comprehensive evaluation of the degree of soil contamination—A review. *Environmental Geochemistry and Health, 40*, 2395–2420. https://doi.org/10.1007/s10653-018-0106-z

Koul, B., Bhat, N., Abubakar, M., Mishra, M., Arukha, A. P., & Yadav, D. (2022). Application of natural coagulants in water treatment: A sustainable alternative to chemicals. *Water, 14*(22), 3751.

Muhaymin, A., Mohamed, H. E. A., Hkiri, K., Safdar, A., Azizi, S., & Maaza, M. (2024). Green synthesis of magnesium oxide nanoparticles using *Hyphaene thebaica* extract and their photocatalytic activities. *Scientific Reports, 14*, 20135.

Oyshi, S. A., Jahan, R. A., Aktar, F., Sultan, M. Z., Chowdhury, A. A., Chowdhury, J. A., Kabir, S., & Amran, M. S. (2025). Preparation and evaluation of the biosynthetic procedure of iron oxide and magnesium oxide nanoparticles using *Hylocereus undatus* fruit peel extract and their anticancer properties. *RSC Advances, 15*(19), 15366–15374. https://doi.org/10.1039/D4RA07411D

Parobali, T., Adjei-Mensah, B., Songuine, T., Yarkoa, T., Karou, S. D., & Eklu-Gadegbeku, K. (2024). Influence of *Citrus sinensis* seed powder on growth performance, morphological and histological development of the small intestine of broiler chickens. *Journal of Applied Poultry Research, 33*(1), 100395.

Qasem, N. A. A., Mohammed, R. H., & Lawal, D. U. (2021). Removal of heavy-metal ions from wastewater: A comprehensive and critical review. *npj Clean Water, 4*, 36.

Rotti, R. B., Sunitha, D. V., Manjunath, R., Roy, A., Mayegowda, S. B., Gnanaprakash, A. P., Alghamdi, S., Almehmadi, M., Abdulaziz, O., Allahyani, M., Aljuaid, A., Alsaiari, A. A., Ashgar, S. S., Babalghith, A. O., Abd El-Lateef, A. E., & Khidir, E. B. (2023). Green synthesis of MgO nanoparticles and their antibacterial properties. *Frontiers in Chemistry, 11*, 1143614.

Sharma, S., & Bhattacharya, A. (2017). Drinking-water contamination and treatment techniques. *Applied Water Science, 7*, 1043–1067.

Unnisa, S. A., & Bi, S. Z. (2018). *Carica papaya* seeds effectiveness as coagulant and solar disinfection in removal of turbidity and coliforms. *Applied Water Science, 8*, 149.

World Health Organization. (2022). *Guidelines for drinking-water quality: Fourth edition incorporating the first and second addenda*. World Health Organization.